Triterpenes from *Momordica balsamina* (African pumpkin): ABCB1 inhibition and synergistic interaction with doxorubicin in resistant cancer cells

Cristina Duarte Silva [a], Cátia Ramalhete [a,b], Gabriella Spengler [c], Silva Mulhovo [d], Joseph Molnar [c], Maria-José U. Ferreira [a,*]

[a] Research Institute for Medicines (iMed.ULisboa), Faculty of Pharmacy, Universidade de Lisboa, Av. Prof. Gama Pinto, 1649-003, Lisbon, Portugal
[b] ATLÂNTICA – Instituto Universitário, Fábrica da Pólvora de Barcarena, 2730-036, Barcarena, Oeiras, Portugal
[c] Department of Medical Microbiology, Albert Szent-Györgyi Health Center and Faculty of Medicine, University of Szeged, Semmelweis Utca 6, 6725, Szeged, Hungary
[d] Centro de Estudos Moçambicanos e de Etnociências, Faculdade de Ciências e Matemática, Universidade Pedagógica, 21402161, Maputo, Mozambique

ARTICLE INFO

ABSTRACT

Aiming at overcoming multidrug resistance (MDR) in cancer, we have been studying *Momordica balsamina,* a vegetable known as African pumpkin. Five undescribed cucurbitane-type triterpenoids (balsaminaepoxide, balsaminatriol, balsaminoic acid, balsaminal, and balsaminol G) along with five known cucurbitacins were isolated from the methanol extract of *Momordica balsamina* aerial parts, whose structures were elucidated by spectroscopic data, mainly 1D and 2D NMR experiments. Compounds were evaluated for their ability as P-glycoprotein (P-gp/ABCB1) inhibitors in multidrug resistant human *ABCB1*-transfected mouse lymphoma cells (L5178Y, MDR) and resistant human colon adenocarcinoma cells (COLO 320), using the rhodamine-123 exclusion test, by flow cytometry. Several compounds, which were found to be non-cytotoxic, strongly inhibited P-gp efflux activity in a dose-dependent manner in both cell models. In MRD mouse lymphoma cells, balsaminol G and karavilagenin B were the most active, while in resistant colon adenocarcinoma cells, the strongest inhibitory activity was found for balsaminaepoxide, balsaminatriol and karavilagenin C, being several-fold more active than the positive control verapamil. In chemosensitivity assays, in a model of combination chemotherapy, selected compounds showed to interact synergistically with doxorubicin, thus substantiating their potential as MDR reversers. The strongest synergistic interaction was found for balsaminal and balsaminol G.

1. Introduction

The genus *Momordica* L. (Cucurbitaceae) comprises more than 50 species distributed in the warm tropics, mainly in Africa and Southeast Asia (Bharathi and John, 2013). *Momordica balsamina* L., also known as African pumpkin, balsam apple or southern balsam pear, is widespread in tropical and subtropical regions. Characterized by high nutritional content (Thakur et al., 2009), namely proteins, carbohydrates and minerals, *M. balsamina* is considered a gifted food for poor rural communities where the leaves and fruits are cooked and eaten as a vegetable (Flyman and Afolayan, 2007; Hassan and Umar, 2006). In addition, *M. balsamina* has been widely used in African traditional medicine for the symptomatic treatment of diseases such as diabetes and malaria (Benoit-Vical et al., 2006).

Triterpenes with the cucurbitane skeleton are the most characteristic secondary metabolites from *Momordica* genus (Chen et al., 2005; Kaushik et al., 2015; Shah et al., 2014). These compounds are known to have many biological activities (Chen et al., 2005), namely anticancer and anti-inflammatory properties (Ren and Kinghorn, 2019).

Cancer is a leading cause of death globally. Multidrug resistance (MDR) is often the principal obstacle to the success of chemotherapy. One of the most important mechanisms of MDR is the overexpression of ABC-transporter proteins, which act as efflux pumps. The three major ABC proteins associated with MDR are P-glycoprotein (P-gp/ABCB1), multidrug resistance-associated protein 1 (MRP1/ABCC1) and breast cancer resistance protein (BCRP/ABCG2), the first being the most frequently implicated in MDR. The development of compounds able to inhibit P-gp efflux-activity, hence re-establishing the accumulation of

anticancer agents in cancer cells, has been considered an important strategy for reversing MDR (Stefan, 2019).

In our previous studies, we have isolated several structurally related cucurbitane-type triterpenoids from the aerial parts of *M. balsamina* (Mónico et al., 2019; Ramalhete et al., 2009a, 2009b, 2010, 2011a, 2011b). Most of them, including acyl derivatives, were shown to be potent MDR reversers by inhibiting P-gp efflux-pump activity (Mónico et al., 2019; Ramalhete et al., 2009b, 2016). Additionally, when evaluated for their antiproliferative activity against sensitive cancer cells and corresponding multidrug resistant sublines, using as models gastric, pancreatic and colon cancer entities, some of these compounds were able to selectively kill resistant cancer cells, thus exhibiting collateral sensitivity effect (Ramalhete et al., 2018), which is thought to be among the most promising strategies for tackling MDR. More recently, three triterpenoids, sharing a new 5/6/3/6/5-fused pentacyclic carbon skeleton, named cucurbalsaminane, were isolated from *M. balsamina*. They also displayed strong MDR-reversing activity (Mónico et al., 2019).

Therefore, based on these promising results and aiming at finding effective plant-derived compounds with anti-MDR activity, *e. g* (Cardoso et al., 2021a, 2021b; Ferreira et al., 2018, 2020a, 2020b; Neto et al., 2019; Paterna et al., 2017), we have further studied this species. Thus, herein, we report the isolation and structural elucidation of ten cucurbitane-type triterpenoids (Fig. 1), from the MeOH extract of *M. balsamina,* including five undescribed compounds (**1-5**) along with karavilagenins A – C (**6–8**), and kuguacins B (**9**) and C (**10**). Using human *ABCB1*-gene transfected L5178Y mouse lymphoma cells and resistant human colon adenocarcinoma cells, we report their ability as P-gp inhibitors, along with their cytotoxicity. Additionally, drug combination studies with the anticancer drug doxorubicin were performed.
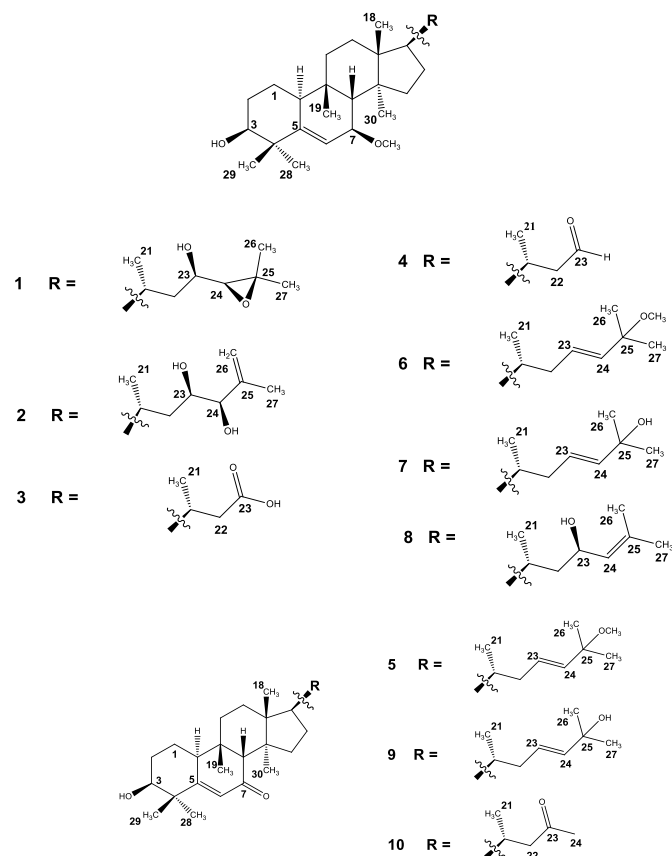

Fig. 1. Structures of compounds **1–10**.

2. Results and discussion

2.1. Chemistry

Fractionation of the ethyl acetate soluble part of the methanol extract (Mónico et al., 2019) of the air-dried powdered aerial parts of *M. balsamina* yielded five undescribed cucurbitacins (**1–5**), together with the known compounds **6–10**, which were identified as karavilagenins A (**6**) (Chang et al., 2008; Nakamura et al., 2006), B (**7**) (Chang et al., 2008; Nakamura et al., 2006) and C (**8**) (Nakamura et al., 2006; Ramalhete et al., 2009b), and kuguacins B (**9**) (Chen et al., 2008) and C (**10**) (Chen et al., 2008) by comparison of their spectroscopic data with those reported in the literature.

Compound **1** was isolated as a white amorphous powder with $[\alpha]_D^{20}$ + 92.1 (*c* 0.1, CHCl$_3$). The IR spectrum revealed an absorption band for a hydroxyl group at 3441 cm^{-1}, while its molecular formula was deduced as C$_{31}$H$_{52}$O$_4$, from its HRESITOFMS spectrum, which showed a sodium adduct ion at *m/z* 511.37696 [M + Na]$^+$ (calcd for C$_{31}$H$_{52}$O$_4$Na, 511.37578), consistent with six degrees of unsaturation. The ^{1}H NMR spectrum (Table 1) showed proton resonances corresponding to seven singlets of tertiary methyl groups (δ_H 0.67, 0.90, 0.93, 0,97, 1.15, 1.23, 1.25), a secondary methyl at δ_H 0,89 (3H, *d*, *J* = 6.4 Hz), one methoxy at δ_H 3.28, and four oxymethine protons (δ_H 2.65, *d*, *J* = 8.4 Hz; 3.37, *brd*, *J* = 5.0 Hz; 3.45 *brs* and 3.50, *dd*, *J* = 8.4 and 2.2 Hz). Furthermore, a vinylic NMR signal of a tri-substituted double bound at δ_H 5.77 (*d, J* = 5.0 Hz) was also observed. The ^{13}C NMR spectrum (Table 2) displayed 31 carbon resonances, identified by a DEPT experiment as nine methyl groups (including a methoxy at δ_C 56.2), seven methylenes, nine methines (including one *sp2* at δ_C 120.7, and four oxygenated at δ_C 68.1, 68.3, 76.7 and 77.2), and six quaternary carbons (one *sp^2* at δ_C 146.9 and one oxygenated at δ_C 59.1). The ^{1}H–^{1}H COSY and HMQC spectra allowed the establishment of two spin systems (Fig. 2a), namely (A) –CH(OH)–CH$_2$–CH$_2$–CH–C=CH–CH(OCH$_3$)– and (B) –CH(CH$_3$)–CH$_2$–CH(OH)–CH–, which, together with the heterocorrelations observed in the HMBC spectrum, indicated a triterpene of the cucurbitane-type, having an axially-oriented hydroxyl group at C-3 (based on the small coupling constants of H-3, $J_{3eq, \, 2ax} \cong J_{3eq, \, 2eq}$), a double bond at C-5 and a methoxy at C-7, as karavilagenin C (**8**) (Nakamura et al., 2006; Ramalhete et al., 2009b).

The oxygenated carbon resonances at δ_C 59.1, 68.1 and 68.3, observed in the ^{13}C NMR spectrum, along with two proton signals at δ_H 3.50 (*dd, J* = 8.4, 2.2 Hz), and 2.65 (*d, J* = 8.4 Hz), provided evidence for a hydroxyl group and an epoxide at the side chain, which were located at C-23 and C-24/C-25, respectively, substantiated by the HMBC spectrum through $^2J_{C-H}$ and $^3J_{C-H}$ heteronuclear correlations between H-23 (δ_H 3.50), Me-26 (δ_H 1.23) and Me-27 (δ_H 1.25) with C-24 (δ_C 68.3) and between H-20 (δ_H 1.39) and H-24 (δ_H 2.65) with C-23 (δ_C 68.1).

The relative configuration of the stereocenters of the tetracyclic nucleus of **1** was found to be identical to that of karavilagenin C (**8**) as determined by a NOESY spectrum (Fig. 2b), taking into consideration the coupling constant pattern and cucurbitacins biogenesis (Xu et al., 2004). Concerning the side chain, the configuration at C-23 (*R*) and C-24 (*S*) was substantiated by the Nuclear Overhauser effects observed between H-23 and H-24, together with their coupling constant values [H-23 (*J* = 8.4, 2.2 Hz) and H-24 (*J* = 8.4 Hz)], which were similar to those found for alisol B, a protostane-type triterpenoid that shares the same side chain (Jin et al., 2012; Nakajima et al., 1994). Therefore, compound **1** was determined to be 24(*S*),25-epoxy-7β-methoxycucurbit-5-ene-3β,23(*R*)-diol, and named balsaminaepoxide.

Compound **2** was isolated as a white powder with $[\alpha]_D^{20}$ + 79.1 (*c* 0.1, CHCl$_3$) molecular formula, C$_{31}$H$_{52}$O$_4$, as inferred from its HRESITOFMS spectrum through the ion at *m/z* 511.37739 [M + Na]$^+$ (calcd for C$_{31}$H$_{52}$O$_4$Na, 511.37578). When comparing the NMR data of compound **2** with those of **1**, it could be concluded that they shared the same triterpenic nucleus, differing only in the C-17 side chain. Therefore, besides the signals corresponding to the tetracyclic scaffold, the NMR data

Table 1
^{1}H NMR data for compounds **1–5** (δ in ppm, *J* in Hz, 300 MHz).[a]

No.	1[b]	2[b]	3[c]	4[b]	5[b]
	δ_H (*J* in Hz)				
1	1.42, m; 1.56, m	1.56, m	1.42, m; 1.70, m	1.14, m; 1.59, m	1.72, m
2	1.73, m; 1.91, m	1.74, m; 1.88, m	1.61, m; 1.69, m	1.74, m	1.82, m; 1.98, m
3	3.45, brs	3.50, bs	3.37, bs	3.51, bs	3.64, bs
6	5.77, d (5.0)	5.81, d (4.7)	5.88, d (4.9)	5.84, d (4.6)	6.08, d (2.1)
7	3.37, brd (5.0)	3.41, bd (5.4)	3.33, d (5.3)	3.41, d (5.3)	–
8	1.99, d (3.0)	2.04, bs	2.08, s	2.05, bs	2.40, s
10	2.21, dd (11.0, 6.0)	2.26, dd (11.8; 5.1)	2.14, m	2.27 dd (11.8, 5.3)	2.70, td (7.4, 1.8)
11	1.39, m; 1.61, m	1.49, m; 1.61, m	1.39, m; 1.53, m	1.63, m	1.45, m; 1.78, m
12	1.44, m; 1.64, m	1.53, m	1.29, m; 1.39, m	1.30, m; 1.66, m	1.60, m; 1.73, m
15	1.30, m	1.31, m	1.18, m	1.20, m; 1.35, m	1.57, m; 1.06, m
16		1.33, m; 1.87, m	1.64, m; 1.73, m	1.33, m; 1.89, m	1.35, m; 1.88, m
17	1.36, m	1.42, m	1.38, m	1.49, m	1.45, m
18	0.90, s	0.94, s	0.81, s	0.97, s	0.87, s
19	0.93, s	0.91, s	1.20, s	1.00, s	0.96, s
20	1.39, m	1.73, m	2.01, m	2.13, m	1.54, m
21	0.89, d (6.4)	0.92, d (6.4)	1.05, d (6.0)	0.98, d (6.6)	0.89, d (6.1)
22	0.88, m; 1.69, m	0.93, m; 1.52, m	1.96, m; 2.38, m	2.13, m; 2.46 dd (15.0, 4.1)	1.78, m; 2.17, m
23	3.50, dd (8.4, 2.2)	3.67, ddd (10.9,6.6,1.9)	–	9.75, brs	5.49, ddd (15.6,8.1,5.4)
24	2.65, d (8.4)	3.77, d (6.6)	–	–	5.37, d (15.6)
25	–	–	–	–	–
26	1.23, s	4.98,bs; 4.93,bs	–	–	1.23, s
27	1.25, s	1.71,s	–	–	1.23, s
28	0.97, s	1.01, s	0.92, s	1.03, s	1.13, s
29	1.15, s	1.19, s	1.17, s	1.21, s	1.24, s
30	0.67, s	0.69, s	0.59, s	0.71, s	0.81, s
7-OMe	3.28, s	3.32, s	3.24, s	3.34, s	–
25-OMe	–	–	–	–	3.13, s

[a] Assignments were based on DEPT, HMQC, COSY, and HMBC experiments.
[b] Data were recorded in $CDCl_3$.
[c] Data were recorded in C_6D_6.

Table 2
^{13}C NMR spectroscopic data for compounds **1–5**. (δ in ppm, 75 MHz)[a].

No.	1[b]	2[b]	3[c]	4[b]	5[b]
1	21.1	21.2	21.4	21.2	21.0
2	28.7	28.7	29.3	28.7	28.8
3	76.7	76.9	76.6	76.9	76.8
4	41.7	41.9	41.8	41.9	42.9
5	146.9	146.9	146.7	147.0	169.2
6	120.7	121.0	120.9	121.0	126.0
7	77.2	77.4	77.3	77.4	203.0
8	47.8	47.9	48.8	48.1	59.9
9	33.9	34.1	34.3	34.1	36.0
10	38.7	38.8	39.1	38.8	40.4
11	32.7	32.8	32.9	32.7	31.4
12	30.2	30.3	30.4	30.2	29.9
13	46.2	46.3	46.3	46.4	45.8
14	47.9	48.0	48.3	48.1	48.6
15	34.6	34.7	34.9	34.7	34.7
16	27.8	28.0	27.9	28.1	27.9
17	50.9	51.0	50.3	50.3	49.7
18	15.4	15.5	15.4	15.5	15.5
19	28.8	29.0	29.3	29.0	28.0
20	31.9	32.6	34.1	32.0	36.3
21	18.6	18.6	19.8	20.2	19.0
22	40.2	39.8	41.7	51.3	39.5
23	68.1	69.6	178.6	203.6	128.5
24	68.3	80.3	–	–	136.9
25	59.1	144.8	–	–	75.0
26	19.1	114.2	–	–	26.2
27	25.0	18.0	–	–	25.9
28	27.8	27.8	27.9	27.9	28.0
29	25.4	25.5	25.7	25.5	25.0
30	18.0	18.1	18.2	18.1	18.1
7-OMe	56.2	56.4	56.2	56.4	–
25-OMe	–	–	–	–	50.4

[a] Assignments were based on DEPT, HMQC, COSY, and HMBC experiments.
[b] Data were recorded in $CDCl_3$.
[c] Data were recorded in C_6D_6.

of **2** (Table 1) indicated the presence of one allylic tertiary methyl group, (δ_H 1.71), two oxygenated methines (δ_H 3.67 and 3.77; δ_C 69.6 and 80.3) and a terminal double bond (δ_H 4.93, *brs*; 4.98, *brs*; δ_C 144.8 and 114.2). Detailed analysis of the ^{1}H–^{1}H COSY and HMQC spectra of **2** substantiated these structural features, allowing to deduce the side chain as –CH(CH₃)–CH₂–CH(OH)–CH(OH)–C(CH₃)=CH₂ where the position of the functional groups was supported by the HMBC spectrum. In this way, $^3J_{H-C}$ and $^2J_{H-C}$ long-rang correlations between H-24 and C-22/C-23/C-25/C-26/C-27 provided evidence for a diol system at C-23 and C-24, and the terminal double bond was corroborated by the $^3J_{H-C}$ correlation between Me-27 and C-26. The relative configuration of the side chain stereocenters of **2**, namely the diol system at C-23/C-24, was deduced based on the coupling constant values of H-23 and H-24 [H-23 (*J* = 10.9, 6.6, 1.9 Hz); H-24 (*J* = 6.6 Hz)], which were identical to those reported for the tetracyclic triterpene alisol G, bearing a cycloartane scaffold and the same side chain [H-23 (*J* = 10.7, 6.5, 1.7 Hz); H-24 (*J* = 6.5 Hz)] (Yoshikawa et al., 1993). The NOE cross-peaks observed between Me-21/H-23, H-23/Me-27 and Me-27/H-24 substantiated the assignment. Thus, the structure of **2** was determined to be 7β-methoxycucurbita-5,25-diene-3β,23(R),24(R)-triol, and named balsaminatriol.

Compound **3** was isolated as a white amorphous powder, $[\alpha]_D^{23}$ + 49.5. Its IR spectrum showed absorption bands of carboxyl and hydroxyl functions at 3422 cm^{-1} and 1703 cm^{-1}, respectively. Its molecular formula, $C_{27}H_{44}O_4$, consistent with six degrees of unsaturation, was deduced from its HRESITOFMS spectrum that exhibited a sodium adduct ion at *m/z* 455.31404 [M + Na]$^+$ (calcd for $C_{27}H_{44}O_4Na$: 455.31318). The ^{1}H NMR and ^{13}C NMR data of compound **3** (Tables 1 and 2) were similar to those of compounds **1** and **2**, having however only 27 signals in the ^{13}C NMR spectrum. In effect, the carbon signals assignable to the side chain from C-24 to C-27, as well as the corresponding proton resonances in the ^{1}H NMR spectrum, were absent, indicating for compound **3** a *nor*-cucurbitane-type scaffold. In the ^{13}C NMR data, seven methyls (being one a methoxy), seven methylenes, seven methines and six quaternary carbons were observed. Extensive analysis of the 2D NMR data
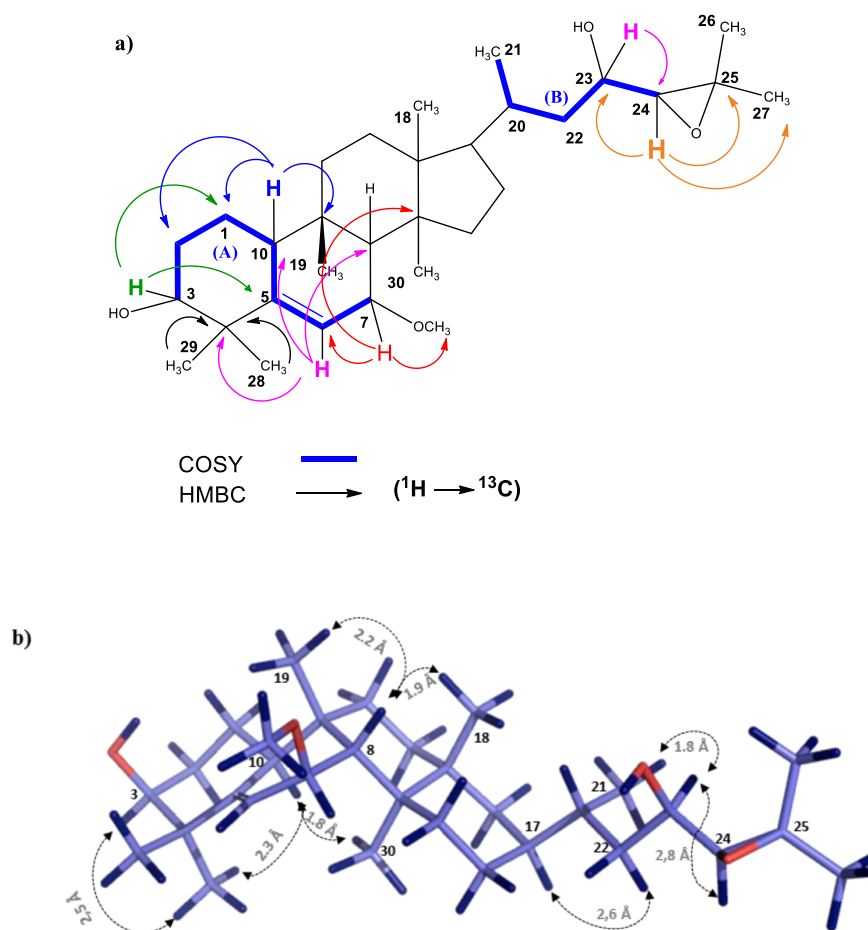
Fig. 2. Key (a) ^{1}H–^{1}H COSY, HMBC and (b) NOESY correlations of balsaminaepoxide (**1**). Energy minimization of the 3D structure of **1** was carried out in MOE (Molecular Operating Environment) through the MOPAC semi-empirical quantum chemistry program, using the PM3 Hamiltonian and a root mean square gradient at 0.01 kcal/mol/A^2. PyMOL was used to visualize the pictures of the models of **1**.

of **3** allowed the assignment of the side chain fragment: –CH(CH$_3$)– CH$_2$–COOH. The presence of a carboxylic acid group at C-23 was sub-stantiated by the HMBC correlations between H-20 (^3J) and H-22 (^2J) with C-23. Taken together with the NOESY spectrum, the structure of compound **3** was determined to be 24,25,26,27-*tetranor*-7β-methox-ycucurbit-5-ene-3β-hydroxy-23-oic acid, and named balsaminoic acid.

Compound **4**, isolated also as a white amorphous powder, bears a molecular formula of C$_{27}$H$_{44}$O$_3$, as determined by HRESITOFMS *m/z* 417.33678 [M + H]$^+$ (calcd for C$_{27}$H$_{45}$O$_3$ 417.33632). Its IR spectrum showed absorption bands of hydroxyl and carbonyl groups at 3418 cm^{-1} and 1717 cm^{-1}, respectively. When comparing the NMR data of **4** (Ta-bles 1 and 2) with those of compound **3**, the carboxylic group at C-23 was replaced by an aldehyde function (δ$_H$ 9.75 and δ$_C$ 203.6), which was also supported by the strong paramagnetic effect ($\approx$ 10 ppm) observed at C-22 (δ$_C$ 51.3), as expected (α-carbon). In the HMBC spectrum, the $^2J_{C-H}$ correlation from H-22 (δ$_H$ 2.46 (*dd*, *J* = 15.0; 4.1 Hz) and 2.13 *m*)] to C-23 (δ$_C$ 203.6) also corroborated the above assignment. Similar NOESY correlations to those observed for compounds **1–3** supported the relative configuration of the tetracyclic scaffold of **4**, which was established as 24,25,26,27-*tetranor*-7β-methoxycucurbit-5-ene-3β-hydroxy-23-al, named balsaminal.

Compound **5** exhibited a protonated molecule at m/z 471.38403 [M + H]$^+$ in the HRESITOFMS spectrum, corresponding to the molecular formula C$_{31}$H$_{50}$O$_3$ (calcd for C$_{31}$H$_{51}$O$_3$: 471.38327). The IR spectrum displayed absorption bands for a hydroxyl function and a conjugated carbonyl group at 3447 and 1645 cm^{-1}, respectively. The ^{1}H and ^{13}C NMR spectra of **5** showed resonances for seven tertiary methyl groups

(Tables 1 and 2), a secondary methyl (δ$_H$ 0.89 *d*, *J* = 6.1 Hz; δ$_C$ 19.0), a methoxy group (δ$_H$ 3.13; δ$_C$ 50.4), one oxygenated methine (δ$_H$ 3.64 *brs*; δ$_C$ 76.8), a di-substituted double bound (δ$_H$ 5.49 *dd*, *J* = 15.6, 8.1, 5.4 Hz and δ$_H$ 5.37 *d*, *J* = 15.6 Hz; δ$_C$ 128.5 and 136.9), and an α,β-unsaturated carbonyl system (δ$_H$ 6.08 *d*, *J* = 2.1 Hz; δ$_C$ 126.0, 169.2 and 203.0). The HMBC $^2J_{C-H}$ correlation from H-8 (δ$_H$ 2.40) to C-7 (δ$_C$ 203.0) and the strong paramagnetic effects observed at C-5 (δ$_C$ 169.2, Δδ $\approx$ +22), owing to mesomeric effects, supported the presence of the enone feature in ring B. As a result, the structure of **5** was elucidated as 25-methox-ycucurbita-5,23(*E*)-diene-3β-hydroxy-7-one, and named balsaminol G.

2.2. Cytotoxic activity of compounds

The cytotoxic activity of compounds **1–10** was assessed on sensitive and resistant human colon adenocarcinoma cells (COLO 205, sensitive; COLO 320, resistant) and on L5178Y parental (L5178Y, PAR) and human *ABCB1*-gene transfected (L5178Y, MDR) mouse T-lymphoma cells through the thiazolyl blue tetrazolium bromide (MTT) assay (Table S1, Supporting Information). As displayed in Table S1 (Sup-porting Information), the compounds were non-cytotoxic or showed weak cytotoxicity in both cell lines and corresponding sublines (IC$_{50}$ > 25 μM in colon adenocarcinoma cells line and IC$_{50}$ > 28 μM in mouse T-lymphoma cells).

2.3. P-gp-mediated MDR reversal activity

Compounds **1–10** were assessed for their ability as P-gp inhibitors,

by the standard rhodamine-123 functional assay, on both sensitive mouse T-lymphoma and human colon adenocarcinoma cell lines and corresponding MDR sublines. The inhibition of P-gp efflux activity is given by fluorescence activity ratio (FAR), which represents the accumulation of rhodamine-123 between resistant (COLO 320 and L5178Y-MDR) and sensitive (COLO 205 and L5178Y-PAR) cells. All the compounds were tested at 2 and 20 μM, and in some cases (**5**, **7**, **8**) at 0.2 μM. Verapamil was used as positive control (20 μM). In the human *ABCB1-* gene transfected mouse lymphoma cells, compounds with FAR values higher than 1 are classified as active P-gp inhibitors and those with FAR values > 10 as strong inhibitors. The same classification cannot be applied in COLO 320 MDR cells owing to their lower P-gp expression values.

The results are summarized in Table 3. As it can be observed, in mouse lymphoma cells, excepting compound **3**, which was barely active, all the compounds revealed to inhibit strongly the P-gp efflux activity at the highest concentration tested (20 μM), exhibiting balsaminol G (**5**) and karavilagenin B (**7**) the highest FAR values (137.8 and 91.3, respectively). In the same way, compounds **5**, and **7** were also the strongest inhibitors at 2 μM (FAR = 14.8, 40.4, respectively), being more active than the positive control verapamil, at ten-fold higher concentration (FAR = 6.6 at 20 μM). A strong activity was also previously found for compound **8** (FAR = 42.0) at 2 μM (Ramalhete et al., 2009b).

Similarly, in the human resistant COLO 320 adenocarcinoma cells, in spite of being observed a decrease on FAR values, compounds **5**, **7** and **8** were also among the most active, acting in a dose dependent effect (FAR values ranging from 1.9 to 3.4 at 2 μM, and from 14.7 to 21.8 at 20 μM). However, the strongest FAR values at 20 μM were found for compounds **1** (FAR = 3.5 and 23.8, at 2 and 20 μM, respectively) and **2** (FAR = 3.1 and 29.8, at 2 and 20 μM, respectively). When compared with verapamil (FAR = 4.0 at 20 μM), compounds **1** and **2** were six and seven-fold more active, respectively (at 20 μM).

The compounds (**1–10**) share the cucurbitane skeleton, having compounds **1–4** and **6–8** a methoxy group at C-7, whereas compounds **5**, **9** and **10** bear a ketone group at this position integrated in an enone system. When comparing the results of compounds from the first set (**1–4** and **6–8**), the presence of hydroxyl groups at the side chain appears to play an important role in reversing MDR activity on both cell lines (**7**, FAR = 40.4 and 91.3 at 2 and 20 μM, respectively - L5178Y-MDR; FAR = 3.4 and 18.2 at 2 and 20 μM, respectively -COLO 320). It is interesting to note that the *nor*-cucurbitanes **3** and **4** showed a marked decrease of FAR values (at 2 μM), highlighting the importance of the side chain for the activity in both cell lines. This conclusion was substantiated by the results observed for the *nor*-cucurbitane **10**, with a carbonyl group at C-7. In fact, in these three compounds, bearing an α,β-unsaturated carbonyl group in ring B (**5**, **9** and **10**), compounds **5** and **9**, which differ from **10** only in the side chain, showed a higher activity in both cell lines (Table 3). These results are in agreement with those that we have previously found for other *nor*-cucurbitane-type triterpenoids (Mónico et al., 2019; Ramalhete et al., 2009b, 2016).

Aiming at finding correlation between FAR values obtained in the transport assay and some physicochemical properties of compounds **1–10**, the molecular descriptors molecular weight (MW), molecular volume (MV), logarithm of the octanol/water partition coefficient (log *P*), topological polar surface area (TPSA) and hydrogen-bonding potential were calculated, using Molinspiration Cheminformatics free web services and Virtual Computational Chemistry Laboratory software (Table S2) (Molinspiration, 2021; Tetko et al., 2005; VCCLAB, 2021). By analysis of Table S2 of compounds **1–10**, although no statistical correlation with FAR values was found, it could be observed that the most active compounds (**5** and **7**) on L5178Y mouse lymphoma cells were among the most lipophilic (log *P* values of 7.0 and 6.7, respectively). They are characterized by TPSA values of 46.5 and 49.7 Å², respectively, molecular weight of 470 (**5**) and 472 (**7**) g/mol, and a similar molecular volume (**5**, 493.4 Å³; **7**, 499.3 Å³). Moreover, they can establish four or five hydrogen bonds. Conversely, when comparing the physicochemical

properties of compounds **1** and **2**, which showed the best activity on the human colon adenocarcinoma cells, it is interesting to note that they are among the compounds with the lowest log *P* values (5.2 and 5.0, respectively). Moreover, they showed the highest molecular weight (488 g/mol), TPSA values (**1**, 62.2 Å²; **2**, 69.9 Å²) and H-bonding potential (7 and 6 hydrogen bonds). The molecular volume of both compounds was also among the highest observed (**1**, 503.7 Å³; **2**, 508.2 Å³). Based on these results, it can be deduced that the inhibition of P-gp efflux activity of these compounds depends on several factors, including the intrinsic characteristics of the studied cell lines.

2.4. Combination assay with doxorubicin

In order to study the type of *in vitro* interaction between the test compounds (excepting compounds **3** and **10**) and the anticancer drug doxorubicin, they were evaluated in a combination chemotherapy model on MDR mouse T-lymphoma cells. On the assay, several concentrations of compounds and doxorubicin were used and the extension of interactions between doxorubicin and the tested compound was calculated and expressed using the combination index (CI) value defined by Chou and Talalay (Chou, 2010). As it can be observed in Fig. 3, all the compounds displayed a synergistic interaction with doxorubicin, showing balsaminol G (**5**), and balsaminal (**4**) the strongest interaction (CI value of 0.29) with doxorubicin. Interestingly, compound **5** showed the highest FAR value in the transport assay at 20 μM (FAR = 137.8) with the same cell line.

Doxorubicin is a P-gp substrate. Therefore, the efficacy of this anticancer drug, which is used to treat many types of solid and haematological tumours, has been hampered by P-gp overexpression, which affects the pharmacokinetics of doxorubicin and thus contributes to drug resistance. The clinical use of this anticancer drug has been limited by its side effects, one of the most serious being its toxicity to the cardiac muscle, where P-gp expression level is variable. Doxorubicin efficacy and toxicity has been reported to depend on the expression and function of ABC efflux proteins, such as P-gp, and cation uptake transporters (Otter et al., 2022). Thus, intracardiac concentrations of various compounds may be modified, depending on the individual P-gp level.

3. Conclusions

Cucurbitane-type triterpenoids from the *M. balsamina* were previously reported by our group as promising P-gp inhibitors. Therefore, aiming at finding new active compounds for structure-activity relationship studies, we have further investigated this species. Five undescribed cucurbitane-type triterpenoids (**1–5**), along with five known cucurbitacins (**6–10**), were isolated and assessed for their ability as MDR reversers on multidrug resistant mouse T-lymphoma and human colon adenocarcinoma cell lines, using both functional and chemosensitivity assays. In human transfected mouse lymphoma cells, the most active compounds were balsaminol G (**5**) and karavilagenin B (**7**), which were many-fold more active than the positive control verapamil. However, all compounds, expecting **3**, were found to be very strong inhibitors at 20 μM. In combination assays in the same cell line, these compounds, which were found non-cytotoxic, interacted synergistically with the anticancer drug doxorubicin, corroborating the results obtained in the transport assay. In turn, in human resistant COLO 320 adenocarcinoma cells, the strongest FAR values were found for compounds **1**, **2**, and **8**, which were five to seven-fold more active than verapamil at 20 μM.

4. Experimental

4.1. General procedures

Optical rotations were obtained using a PerkinElmer 241 polarimeter. Infrared spectra were taken on an Affinity-1 (Shimadzu) FTIR infrared spectrophotometer. NMR spectra were recorded on a Bruker
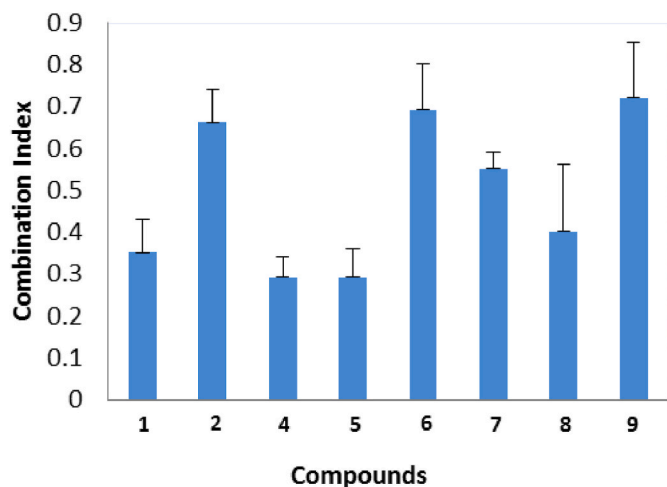
Table 3

Effects of compounds **1–10** on P-gp mediated R123 efflux, in *ABCB1*-transfected mouse T-lymphoma (L5178Y-MDR) cells and in resistant human colon adenocarcinoma cells (COLO 320).

1-4, 6-8

5, 9, 10

compound	FAR[a]			
	R	concentration μM	L5178Y-MDR	COLO 320
Balsaminaepoxide (**1**)		2.0	9.7	3.5
		20.0	70.9	23.8
Balsaminatriol (**2**)		2.0	5.1	3.1
		20.0	74.0	29.8
Balsaminoic acid (**3**)		2.0	1.1	1.2
		20.0	1.6	1.6
Balsaminal (**4**)		2.0	1.4	0.7
		20.0	58.2	4.9
Balsaminol G (**5**)		0.2	1.0	–
		2.0	14.8	1.9
		20.0	137.8	14.7
Karavilagenin A (**6**)		2.0	7.0	1.7
		20.0	55.0	7.4
Karavilagenin B (**7**)		0.2	1.1	–
		2.0	40.4	3.4
		20.0	91.3	18.2
Karavilagenin C (**8**)[b]		0.5	1.5	–
		1.0	15.0	–
		2.0	42.0	3.1
		20.0	46.0	21.8
Kuguacin B (**9**)		2.0	6.1	1.6
		20.0	57.0	7.6
Kuguacin C (**10**)		2.0	1.5	1.4
		20.0	16.4	2.2
Verapamil	–	20.0	6.7	4.0
DMSO	–	2.0%	1.1	

[a] FAR = $(MDR_{treated}/MDR_{control})/(Parental_{treated}/Parental_{control})$.

[b] The results for karavilagenin C (**8**) were obtained previously (Ramalhete et al., 2009b).

Fig. 3. Evaluation of the interaction between selected compounds (**1**, **2**, **4–9**) and doxorubicin on *ABCB1*-transfected mouse T-lymphoma (L5178Y - MDR) cells. Combination index (CI) values presented in the picture are the mean ± standard deviation (SD) for an inhibitory concentration of 50 % (IC$_{50}$). 0.1 < CI < 0.3: strong synergy; 0.3 < CI < 0.7: synergy; 0.7 < CI < 0.9: moderate to slight synergy; 0.9 < CI < 1.1 nearly additive; 1.10 < CI < 1.45: moderate antagonism; 1.45 < CI < 3.30: antagonism (Chou, 2006).

Advance 300 NMR spectrometer (^{1}H 300 MHz; ^{13}C 75 MHz), using CDCl$_3$ as solvent. ^{1}H and ^{13}C chemical shifts are expressed in δ (ppm) referenced to the solvent used and the proton coupling constants *J* are in hertz (Hz). High-resolution mass spectra (HRMS) were recorded on a FTICR-MS Apex Ultra (Brüker Daltonics) Tesla mass spectrometer. Column chromatography (CC) was carried out on SiO$_2$ (Merck 9385) or Combiflash system (Teledyne-Isco; Lincoln, NE, USA), using SiO$_2$ or C$_{18}$ pre-packed columns. TLC was performed on pre-coated SiO$_2$ F$_{254}$ plates (Merck 5554 and 5744) and visualized under UV light and by spraying with sulfuric acid-methanol (1:1) followed by heating. HPLC was done on a Merck-Hitachi instrument, with UV detection (254 nm), using a Merck LiChrospher 100 RP-18 (10 μm × 250 mm × 10 mm) column.

4.2. Plant material

The aerial parts of *Momordica balsamina* L. (Cucurbitaceae) were collected in Gaza, Mozambique (Latitude: 23° 44′ S; Longitude: 32° 44′ E), in November 2015 (wet season). The plant material was identified by Prof. Silva Mulhovo. A voucher specimen (30 SM) has been deposited at the herbarium (LMA) of the Instituto de Investigação Agronómica, Maputo, Mozambique.

4.3. Extraction and isolation

The air-dried powdered aerial parts of *M. balsamina* (4.5 kg) were extracted exhaustively with methanol (8 × 15 L), at room temperature. After evaporating the methanol, at 40 °C, it was obtained a residue of 865 g, which was suspended in MeOH–H$_2$O solution (1:2) and extracted with EtOAc. The resulting crude EtOAc extract was dried (Na$_2$SO$_4$) and evaporated, yielding a residue of 535 g that was chromatographed over silica gel (3 kg), with mixtures of *n*-hexane-EtOAc and EtOAc-MeOH of increasing polarity, giving rise to eight fractions (fraction A-H), after TLC analysis.

Fraction E (27.0 g), obtained with *n*-hexane-EtOAc (3:2), was chromatographed using a silica gel column, yielding fifteen fractions (F$_{E1}$-F$_{E15}$). Fraction F$_{E7}$ (8.2 g, *n*-hexane-EtOAc; 3:2 to 1:1), yielded 2.2 g of compound **8**, after recrystallization (*n*-hexane–EtOAc). The mother liquors residue of F$_{E7}$ (6.0 g) was repeatedly chromatographed, over silica gel and silica RP-18, yielding five compounds, namely compounds **1** (148 mg), **2** (133 mg), **3** (32 mg), **6** (32 mg) and compound **7** (22 mg),

whereas compound **4** (10 mg) was obtained after further purification by semi-preparative HPLC (MeOH–H$_2$O; 4:1).

Fraction F$_{E9}$ (4.3 g, *n*-hexane-EtOAc; 1:1 to 3:2) was fractionated on a Combiflash system (silica RP 18), with H$_2$O–MeOH (1:0 to 0:1; 8 mL/min), giving rise to nine fractions (F$_{E9. A}$ – F$_{E9. I}$). Compound **10** (75 mg) was obtained from fraction F$_{E9. D}$ (658 mg; H$_2$O– MeOH; 1:3) by using a Combiflash system (*n*-hexane-AcOEt and AcOEt-MeOH), and further purification by recrystallization (*n*-hexane-AcOEt). Fraction F$_{E9. F}$ (912 mg; H$_2$O–MeOH; 3:17) was subjected to column chromatography, twice, affording 23 mg and 35 mg of compounds **5** and **9**, respectively.

4.4. Spectroscopic data

Balsaminaepoxide *[24(S),25-epoxy-7β-methoxycucurbit-5-ene-3β,23 (R)-diol]* (**1**): amorphous white powder; [α]$_D^{20}$ + 92.1 (*c* 0.1, CHCl$_3$); IR (NaCl) v$_{max}$ 3441, 2955, 29 230, 2874, 1659, 1456, 1381, 1084, 756 cm^{-1}; ^{1}H and ^{13}C NMR, see Tables 1 and 2; HRESITOFMS *m/z* 511.37696 [M + Na]$^+$ (calcd for C$_{31}$H$_{52}$O$_4$Na, 511.37578).

Balsaminatriol *[7β-methoxycucurbita-5,25-diene-3β,23(R),24(R)-triol]* (**2**): amorphous white powder; [α]$_D^{20}$ + 79.1 (*c* 0.1, CHCl$_3$); IR (NaCl) v$_{max}$ 3405, 2951, 2874, 1655, 1466, 1454, 1381, 1082, 936, 758 cm^{-1}; ^{1}H and ^{13}C NMR, see Tables 1 and 2; HRESITOFMS *m/z* 511.37739 [M + Na]$^+$ (calcd for C$_{31}$H$_{52}$O$_4$Na, 511.37578).

Balsaminoic acid *(24,25,26,27-tetranor-7β-methoxycucurbit-5-ene-3β-hydroxy-23-oic acid)* (**3**): Amorphous white powder; [α]$_D^{23}$ + 49.5 (*c* 0.1, MeOH); IR (NaCl) v$_{max}$ 3422, 2951, 2874, 1703, 1643, 1454, 1383, 1080, 756 cm^{-1}; ^{1}H and ^{13}C NMR, see Tables 1 and 2; HRESITOFMS *m/z* 455.31404 [M + Na]$^+$ (calcd for C$_{27}$H$_{44}$O$_4$Na, 455.31318).

Balsaminal *(24,25,26,27-tetranor-7β-methoxycucurbit-5-ene-3β-hydroxy-23-al)* (**4**): Amorphous white powder; [α]$_D^{23}$ + 10.2 (*c* 0.1, CHCl$_3$); IR (NaCl) v$_{max}$ 3418, 2955, 2926, 2872, 1717, 1653, 1456, 1379, 1084, 758 cm^{-1}; ^{1}H and ^{13}C NMR, see Tables 1 and 2; HRESITOFMS *m/z* 417.33678 [M + H]$^+$ (calcd for C$_{27}$H$_{45}$O$_3$, 417.33632).

Balsaminol G *(25-methoxycucurbita-5,23(E)-diene-3β-hydroxy-7-one)* (**5**): Amorphous white powder; [α]$_D^{23}$ + 76 (*c* 0.1, CHCl$_3$); IR (NaCl) v$_{max}$ 3447, 2957, 2928, 2874, 1645, 1464, 1379, 1298, 1076, 978, 754 cm^{-1}; ^{1}H and ^{13}C NMR, see Tables 1 and 2; HRESITOFMS *m/z* 471.38403 [M + H]$^+$ (calcd for C$_{31}$H$_{51}$O$_3$, 471.38327).

4.5. Cell lines and cell culture

L5178Y mouse T-lymphoma cells (ECACC catalog no. 87111908, U. S. FDA, Silver Spring, MD, U.S.) were prepared and maintained with colchicine to give rise the MDR line (Choi et al., 1991; Cornwell et al., 1987; Pastan et al., 1988). Both MDR and PAR cell line were cultured in McCoy's 5 A medium supplemented with 10% heat-inactivated horse serum, L-glutamine and antibiotics (penicillin, streptomycin). These cells were then incubated in a humidified atmosphere (5% CO$_2$, 95% air) at 37 °C. Regarding the human colon adenocarcinoma cell lines (COLO 205 sensitive and the resistant COLO 320/MDR-LRP expressing P-gp), namely ATCC-CCL-220.1 (COLO 320), and CCL-222(COLO 205) were purchased from LGC Promochem, Teddington England. The cells were cultured in RPMI 1640 medium supplemented with 10% heat-inactivated fetal bovine serum, 2 mM L-glutamine, 1 mM Na pyruvate, and 100 mM HEPES. The semi adherent human colon cancer cells were detached with 0.25% trypsin and 0.02% EDTA for 5 min at 37 °C.

4.6. Cytotoxicity assay

Prior to evaluation in a rhodamine-123 accumulation assay, the cytotoxic effects of compounds **1–10** were tested in a range of decreasing concentrations (maximum concentration 100 μM), on both mouse lymphoma and human colon adenocarcinoma cell lines, in 96-well flat-bottomed microtiter plates. First, the compounds were diluted in 100 μL of medium. Then, 1 × 10^{-4} cells in 100 μL of medium were added to

each well, with the exception of the medium control wells. The culture plates were initially incubated at 37 C for 24 h, and at the end of the incubation period, 20 μL of MTT (thiazolyl blue tetrazolium bromide. Sigma-Aldrich Chemie GmbH, Steinheim) solution of 5 mg/mL in phosphate-buffered saline (PBS) was added to each well and incubated for another 4 h. Then, 100 μL of 10% SDS (sodium dodecyl sulfate, Sigma) solution (10% in 0.01 N HCl) was added into each well, and the plates were further incubated overnight at 37 C. Cell growth was determined by measuring the optical density (OD) at 550 nm (ref. 630 nm) with a Multiscan EX ELISA reader (ThermoLabsSystems, Cheshire, WA, USA). The percentage of inhibition of cell growth was determined as $100 - [(ODsample - ODmediumcontrol)/(ODcellcontrol - ODmediumcontrol)] \times 100$. In this formula, IC_{50} is defined as the inhibitory dose that reduces the growth of the compound-exposed cells by 50%. The IC_{50} values are expressed as means $\pm$ SD from three experiments.

4.7. Rhodamine-123 accumulation assay

For the rhodamine-123 accumulation assay PAR and MDR mouse T-lymphoma cells or human COLO 205 and COLO 320 colon adenocarcinoma cells were adjusted to a density of 2×10^6 cells/mL, resuspended in serum-free McCoy's 5 A medium or RPMI 1640, respectively, and distributed in 0.5 mL aliquots into Eppendorf centrifuge tubes. Then, aliquots (10 μL) of test compounds were added at various concentrations (2 or 20 μM), and verapamil (positive control, EGIS Pharmaceuticals PLC, Budapest, Hungary) was added at 20 μM. DMSO at 2% was also added as solvent control. The samples were incubated for 10 min at room temperature, after which 10 μL (5.2 mM final concentration) of the indicator rhodamine 123 was added. After 20 min of incubation at 37 °C, the samples were washed twice and resuspended in 0.5 mL phosphate-buffered saline (PBS) for analysis by flow cytometry (Partec CyFlow Space Instrument, Partec GmbH, Münster, Germany). The resulting histograms were evaluated regarding mean fluorescence intensity (FL-1), standard deviation, both forward scatter (FSC) and side scatter (SSC) parameters, and the peak channel of 20 000 individual cells belonging to the total and the gated populations (Supporting Information). The fluorescence activity ratio (FAR) was calculated on the basis of the quotient between FL-1 of treated/untreated resistant cell line (ABCB1-transfected mouse lymphoma or COLO 320 human colon adenocarcinoma cells) over the respective treated/untreated sensitive cell line (PAR mouse lymphoma or COLO 205 human colon adenocarcinoma cells).

4.8. Drug combination assay

The combination assay was performed using a fixed ratio of the test compound across a concentration gradient. Doxorubicin (2 mg/mL, Teva Pharmaceuticals, Budapest, Hungary) was serially diluted in the horizontal direction (14.7–0.1 μM) and the dilution of compounds vertically in a 96-microtiter plate to a final volume of 200 μL of medium per well.

The MDR mouse T-lymphoma and COLO 320 human colon adenocarcinoma cells were then distributed in 100 μL aliquots into wells at a concentration of 2×10^5/mL, and the plates were incubated for 72 h at 37 °C in a CO_2 incubator. At the end of the incubation period, the cell growth was determined by MTT staining method, as described earlier. Drug interactions were assessed according to Chou (Chou, 2006, 2010), using the CalcuSyn v2.2 software. Briefly, each dose-response curve (for individual agents as well as combinations) was fit to a linear model using the median effect equation, in order to obtain the median effect value (corresponding to the IC_{50}) and slope (m). The extent of interaction between drugs was expressed using the combination index, in which a CI value close to 1 indicates additivity, while a CI < 1 is defined as synergy and a CI > 1 as antagonism.

Declaration of competing interest

The authors declare that they have no known competing financial interests or personal relationships that could have appeared to influence the work reported in this paper.

Data availability

No data was used for the research described in the article.

Appendix A. Supplementary data

Supplementary data to this article can be found online at https://doi.org/10.1016/j.phytochem.2022.113354.

References

Benoit-Vical, F., Grellier, P., Abdoulaye, A., Moussa, I., Ousmane, A., Berry, A., Ikhiri, K., Poupat, C., 2006. In vitro and in vivo antiplasmodial activity of Momordica balsamina alone or in a traditional mixture. Chemotherapy 52, 288–292. https://doi.org/10.1159/000095960.

Bharathi, L.K., John, K.J., 2013. Momordica Genus in Asia - an Overview, Momordica Genus in Asia - an Overview. Springer India, New Delhi. https://doi.org/10.1007/978-81-322-1032-0.

Cardoso, David S.P., Kincses, A., Nové, M., Spengler, G., Mulhovo, S., Aires-de-Sousa, J., dos Santos, D.J.V.A., Ferreira, M.J.U., 2021a. Alkylated monoterpene indole alkaloid derivatives as potent P-glycoprotein inhibitors in resistant cancer cells. Eur. J. Med. Chem. 210, 112985 https://doi.org/10.1016/J.EJMECH.2020.112985.

Cardoso, David S.P., Szemerédi, N., Spengler, G., Mulhovo, S., Santos, D.J.V.A., dos Ferreira, M.J.U., 2021b. Exploring the monoterpene indole alkaloid scaffold for reversing P-Glycoprotein-Mediated multidrug resistance in cancer. Pharmaceuticals 14. https://doi.org/10.3390/PH14090862.

Chang, C., Chen, C., Liao, Y., Cheng, H., Chen, Y., Chou, C., 2008. Cucurbitane-type triterpenoids from the stems of Momordica charantia. J. Nat. Prod. 71, 1327–1330. https://doi.org/10.1021/np070532u.

Chen, J., Chiu, M., Nie, R., Cordel, G.A., Qiu, S.X., 2005. Cucurbitacins and cucurbitane glycosides: structures and biological activities. Nat. Prod. Rep. 22, 386–399. https://doi.org/10.1039/b418841c.

Chen, J.C., Lu, L., Zhang, X.M., Zhou, L., Li, Z.R., Qiu, M.H., 2008. Eight new cucurbitane glycosides, kuguaglycosides A-H, from the root of Momordica charantia L. Helv. Chim. Acta 91, 920–929. https://doi.org/10.1002/hlca.200890097.

Choi, K., Frommel, T.O., Stern, R.K., Perez, C.F., Kriegler, M., Tsuruo, T., Roninson, I.B., 1991. Multidrug resistance after retroviral transfer of the human MDR1 gene correlates with P-glycoprotein density in the plasma membrane and is not affected by cytotoxic selection. Proc. Natl. Acad. Sci. USA 88, 7386–7390. https://doi.org/10.1073/PNAS.88.16.7386.

Chou, T.-C., 2010. Drug combination studies and their synergy quantification using the chou-talalay method. Cancer Res. 70, 440–446. https://doi.org/10.1158/0008-5472.CAN-09-1947.

Chou, T.C., 2006. Theoretical basis, experimental design, and computerized simulation of synergism and antagonism in drug combination studies. Pharmacol. Rev. 58, 621–681. https://doi.org/10.1124/pr.58.3.10.

Cornwell, M.M., Pastan, I., Gottesman, M.M., 1987. Certain calcium channel blockers bind specifically to multidrug-resistant human KB carcinoma membrane vesicles and inhibit drug binding to P-glycoprotein. J. Biol. Chem. 262, 2166–2170. https://doi.org/10.1016/S0021-9258(18)61633-3.

Ferreira, R.J., Gajdács, M., Kincses, A., Spengler, G., dos Santos, D.J.V.A., Ferreira, M.J. U., 2020a. Nitrogen-containing naringenin derivatives for reversing multidrug resistance in cancer. Bioorg. Med. Chem. 28, 115798 https://doi.org/10.1016/J.BMC.2020.115798.

Ferreira, R.J., Kincses, A., Gajdács, M., Spengler, G., dos Santos, D.J.V.A, Molnár, J., Ferreira, M.J.U., 2018. Terpenoids from Euphorbia pedroi as multidrug-resistance reversers. J. Nat. Prod. 81, 2032–2040. https://doi.org/10.1021/ACS.JNATPROD.8B00326.

Ferreira, R.J., Spengler, G., Orthaber, A., Santos, D.J.V.A., dos Ferreira, M.J.U., 2020b. Pedrolane, a polycyclic diterpene scaffold containing a bicyclo[2.2.1]heptane system, from Euphorbia pedroi. Org. Lett. 23, 274–278. https://doi.org/10.1021/ACS.ORGLETT.0C03647.

Flyman, M.V., Afolayan, A.J., 2007. Proximate and mineral composition of the leaves of Momordica balsamina L.: an under-utilized wild vegetable in Botswana. Int. J. Food Sci. Nutr. 58, 419–423. https://doi.org/10.1080/09637480701253417.

Hassan, L., Umar, K.J., 2006. Nutritional value of balsam apple (Momordica balsamina L.) leaves. Pakistan J. Nutr. 5, 522–529.

Jin, H.-G., Jin, Q., Ryun Kim, A., Choi, H., Lee, J.H., Kim, Y.S., Lee, D.G., Woo, E.-R., 2012. A new triterpenoid from Alisma orientale and their antibacterial effect. Arch Pharm. Res. (Seoul) 3511 (35), 1919–1926. https://doi.org/10.1007/S12272-012-1108-5.

Kaushik, U., Aeri, V., Mir, S.R., 2015. Cucurbitacins - an insight into medicinal leads from nature. Pharm. Rev. 9, 12–18. https://doi.org/10.4103/0973-7847.156314.

Molinspiration, 2021. Cheminformatics Free Web Services [WWW Document]. URL accessed 12.21.21. https://www.molinspiration.com.

Mónico, A., Ramalhete, C., André, V., Spengler, G., Mulhovo, S., Duarte, M.T., Ferreira, M.J.U., 2019. Cucurbalsaminones A-C, rearranged triterpenoids with a 5/6/3/6/5-fused pentacyclic carbon skeleton from Momordica balsamina, as multidrug resistance reversers. J. Nat. Prod. 82, 2138–2143. https://doi.org/10.1021/acs.jnatprod.9b00019.

Nakajima, Y., Satoh, Y., KatsumataneeOhtsuka, M., TsujiyamaneeMikoshiba, K., Ida, Y., Shoji, J., 1994. Terpenoids of Alisma orientale rhizome and the crude drug alismatis rhizoma. Phytochemistry 36, 119–127. https://doi.org/10.1016/S0031-9422(00)97024-9.

Nakamura, S., Murakami, T., Nakamura, J., Kobayashi, H., Matsuda, H., Yoshikawa, M., 2006. Structures of new cucurbitane-type triterpenes and glycosides, karavilagenins and karavilosides, from the dried fruit of Momordica charantia L. In Sri Lanka. Chem. Pharm. Bull. 54, 1545–1550. https://doi.org/10.1248/CPB.54.1545.

Neto, S., Duarte, N., Pedro, C., Spengler, G., Molnár, J., Ferreira, M.J.U., 2019. Effective MDR reversers through phytochemical study of Euphorbia boetica. Phytochem. Anal. 30, 498–511. https://doi.org/10.1002/PCA.2841.

Otter, M., Csader, S., Keiser, M., Oswald, S., 2022. Expression and functional contribution of different organic cation transporters to the cellular uptake of doxorubicin into human breast cancer and cardiac tissue. Int. J. Mol. Sci. 23, 255. https://doi.org/10.3390/ijms23010255.

Pastan, I., Gottesman, M.M., Ueda, K., Lovelace, E., Rutherford, A.V., Willingham, M.C., 1988. A retrovirus carrying an MDR1 cDNA confers multidrug resistance and polarized expression of P-glycoprotein in MDCK cells. Proc. Natl. Acad. Sci. U.S.A. 85, 4486. https://doi.org/10.1073/PNAS.85.12.4486.

Paterna, A., Kincses, A., Spengler, G., Mulhovo, S., Molnár, J., Ferreira, M.J.U., 2017. Dregamine and tabernaemontanine derivatives as ABCB1 modulators on resistant cancer cells. Eur. J. Med. Chem. 128, 247–257. https://doi.org/10.1016/J.EJMECH.2017.01.044.

Ramalhete, C., Da Cruz, F.P., Lopes, D., Mulhovo, S., Rosário, V.E., Prudêncio, M., Ferreira, M.J.U., 2011a. Triterpenoids as inhibitors of erythrocytic and liver stages of Plasmodium infections. Bioorg. Med. Chem. 19, 7474–7481. https://doi.org/10.1016/j.bmc.2011.10.044.

Ramalhete, C., Lopes, D., Molnár, J., Mulhovo, S., Rosário, V.E., Ferreira, M.J.U., 2011b. Karavilagenin C derivatives as antimalarials. Bioorg. Med. Chem. 19, 330–338. https://doi.org/10.1016/j.bmc.2010.11.015.

Ramalhete, C., Lopes, D., Mulhovo, S., Molnár, J., Rosário, V.E., Ferreira, M.J.U., 2010. New antimalarials with a triterpenic scaffold from Momordica balsamina. Bioorg. Med. Chem. 18, 5254–5260. https://doi.org/10.1016/j.bmc.2010.05.054.

Ramalhete, C., Mansoor, T.A., Mulhovo, S., Molnár, J., Ferreira, M.J.U., 2009a. Cucurbitane-type triterpenoids from the African plant Momordica balsamina. J. Nat. Prod. 72, 2009–2013. https://doi.org/10.1021/np900457u.

Ramalhete, C., Molnár, J., Mulhovo, S., Rosário, V.E., Ferreira, M.J.U., 2009b. New potent P-glycoprotein modulators with the cucurbitane scaffold and their synergistic interaction with doxorubicin on resistant cancer cells. Bioorg. Med. Chem. 17, 6942–6951. https://doi.org/10.1016/j.bmc.2009.08.020.

Ramalhete, C., Mulhovo, S., Lage, H., Ferreira, M.J.U., 2018. Triterpenoids from Momordica balsamina with a collateral sensitivity effect for tackling multidrug resistance in cancer cells. Planta Med. 84, 1372–1379. https://doi.org/10.1055/a-0651-8141.

Ramalhete, C., Mulhovo, S., Molnar, J., Ferreira, M.J.U., 2016. Triterpenoids from Momordica balsamina: reversal of ABCB1-mediated multidrug resistance. Bioorg. Med. Chem. 24, 5061–5067. https://doi.org/10.1016/j.bmc.2016.08.022.

Ren, Y., Kinghorn, A.D., 2019. Natural product triterpenoids and their semi-synthetic derivatives with potential anticancer activity. Planta Med. 85, 802–814. https://doi.org/10.1055/A-0832-2383.

Shah, S., Hussain, M., Aslam, M., Rivera, G., 2014. Natural products; pharmacological importance of family cucurbitaceae: a brief review. Mini-Rev. Med. Chem. 14, 694–705. https://doi.org/10.2174/1389557514666140820113055.

Stefan, S.M., 2019. Multi-target ABC transporter modulators: what next and where to go? Future Med. Chem. 11, 2353–2358. https://doi.org/10.4155/fmc-2019-0185.

Tetko, I.V., Gasteiger, J., Todeschini, R., Mauri, A., Livingstone, D., Ertl, P., Palyulin, V. A., Radchenko, E.V., Zefirov, N.S., Makarenko, A.S., Tanchuk, V.Y., Prokopenko, V. V., 2005. Virtual computational chemistry laboratory – design and description. J. Comput. Mol. Des. 196 19, 453–463. https://doi.org/10.1007/S10822-005-8694-Y.

Thakur, G., Bag, M., Sanodiya, B., Bhadauriya, P., Debnath, M., Prasad, G., Bisen, P., 2009. Momordica balsamina: a medicinal and neutraceutical plant for health care management. Curr. Pharmaceut. Biotechnol. 10, 667–682. https://doi.org/10.2174/138920109789542066.

VCCLAB, 2021. Virtual Computational Chemistry Laboratory [WWW Document]. URL. accessed 12.21.21. http://www.vcclab.org.

Xu, R., Fazio, G.C., Matsuda, S.P.T., 2004. On the origins of triterpenoid skeletal diversity. Phytochemistry 65, 261–291. https://doi.org/10.1016/J.PHYTOCHEM.2003.11.014.

Yoshikawa, M., Hatakeyama, S., Tanaka, N., Fukuda, Y., Yamahara, J., Murakami, N., 1993. Crude drugs from aquatic plants. I. On the constituents of alismatis rhizoma. (1). Absolute stereostructures of alisols E 23-acetate, F, and G, three new protostane-type triterpenes from Chinese alismatis rhizoma. Chem. Pharm. Bull. 41, 1948–1954. https://doi.org/10.1248/CPB.41.1948.